ELSEVIER

Materials Chemistry and Physics 41 (1995) 110–116

MATERIALS CHEMISTRY AND PHYSICS

The effects of $Na_4P_2O_7 \cdot 10H_2O$ addition on the mechanical properties of sintered $Ca_2P_2O_7$ bioceramic

Feng-Huei Lin [a,*], Jen-Ren Liaw [a], Min-Hsiung Hon [b], Cheng-Yi Wang [a]

[a] *Center for Biomedical Engineering, College of Medicine, National Taiwan University, Taipei, Taiwan, ROC*

[b] *Department of Material Sciences and Engineering, National Cheng-Kung University, Tainan, Taiwan, ROC*

Received 27 October 1994; revised 10 April 1995; accepted 12 April 1995

Abstract

From the viewpoint of hard tissue response to implant materials, calcium phosphates are probably the most compatible materials presently known. Thus, during the last few years much attention has been paid to hydroxyapatite and β-tricalcium phosphate as potential biomaterials for bone substitute. However, the disadvantage of all proposed calcium phosphate ceramics is their low mechanical strength. Therefore, the applicability of these materials is restricted to the non-stressed regions. The ultimate good of implantation of biomaterials in the skeleton is to reach full integration of non-living implant with living bone. The material could be used, much as a bone graft, as material itself resorbs or dissolves as bone growth occurs, and the end result is new remolded bone. $Ca_2P_2O_7$ is one of intermediate products of bone mineralized crystal from amorphous calcium phosphates. $Ca_2P_2O_7$ doped with a certain amount of $Na_4P_2O_7 \cdot 10H_2O$ was prepared as the developed material. In this study, $Na_4P_2O_7 \cdot 10H_2O$ was used as a liquid phase sintering additive which was expected to improve the sintering process and promote physiological bioresorbability. Compressive strength and four-point bending strength were measured by the Bionix 858 test system. At the beginning, the mechanical strength proportionally increased with addition of $Na_4P_2O_7 \cdot 10H_2O$ up to 5 wt.%, but thereafter decreased. The microstructure and crystalline identification were analyzed by the techniques of scanning electron microscopy (SEM), electron probe micro-analysis (EPMA), transmission electron microscopy (TEM) and X-ray diffraction (XRD). The relationship between mechanical strength of the sintered bioceramics and $Na_4P_2O_7 \cdot 10H_2O$ dopant is given in terms of the presence of $NaCa(PO_3)_3$, grain growth and abnormal grain coalescence while dopant increased.

Keywords: Bone substitute; Biodegradable ceramics; Liquid phase sintering; Mechanical strength

1. Introduction

The capacity of the human body to regenerate bony components that are lost, damaged or diseased is limited. Consequently, surgeons have long endeavored to find or develop materials that might adequately replace bony tissue, especially mineralized tissues such as bone and teeth. Apart from autologous, homilogous or heterologous bone, many materials including metals, alloys, ceramics, carbons, polymers and composites of materials have been studied for use as implant material. However, only a few materials have been proven to be practical to serve as a useful bone substitute [1,2].

Autogenous bone graft is considered to be the most suitable transplant material, because differences in histocompatibility and the risk of transferring a disease from one individual to another are non-existent. However, removal of the bone graft creates additional surgical trauma, and its supply may not be available in sufficient quantity, particularly during childhood. Moreover, the risks of autograft for all patients are longer operation and anaesthesia, high blood loss, risk of infection, risks of damage to nerves and blood vessels, thrombosis and fracture. Allogenic and xenogenic bone transplants represent the alternatives to autogenic bone transplants for certain indications. However, many problems were generally associated with them such as in vivo resorption, disease transfer, considerable care, high costs and regular provocation of an immuno-defensive reaction, which limits their efficiency, application and availability of the transplant materials [3,4].

To overcome these problems, various artificial materials to fill bone defects have been developed. The ultimate goal of implantation of biomaterials in the skeleton is to reach full integration of non-living implant with living bone. The material could be used, much as a bone graft, as a material itself resorbs or dissolves as bone growth occurs, and the end result is new remolded bone [5]. The requirements center on

* Corresponding author.

SSDI 0254-0584(95)01541-2

resorbability and the lack of toxicity or other harmful effects arising from the release and metabolism of the degeneration products. With advances in ceramic technology, the application of calcium phosphate materials as bone substitute has recently received considerable attention, because they are remarkably biocompatible, provoke little, if any, inflammatory response, and have a bioactive property: direct chemical bonding of bone to the material [6,7].

Having the same chemical composition as the natural bone, the products of calcium phosphate ceramics are regarded as a promising bone substitute material in the orthopedic field. The goal of bone substitute is initially aimed to refill the defective bony structure and it can be finally replaced by the host new bone [4,5]. In order to reach this expectation, the implant has to be bioactive and biodegradable. Most of the products of calcium phosphate ceramics were confirmed bioactive that osteogenic mesenchymal tissues can be attracted and proceed to form new bone. Hydroxyapatite (HA) and tricalcium phosphate (TCP) are two major products commonly used in the conventional market. Because their calcium/phosphate (Ca/P) ratio resembles natural bone, they are mostly stable in the physiological environment. The former, HA, constitutes a major composition of bone materials and is almost non-degradable even after a long period of implantation, while the latter, TCP, is more or less resorbable. Nevertheless, the extent of degradation of TCP mainly depends on its structure. It was reported to be completely resorbed in the powder form, but a similar procedure has only been partially done in the block form. In practice, the granular or block form of the bone substitute is more compatible for clinical use [2,8]. Thus, searching for a new biodegradable ceramics material is the primary goal of this study.

HA and other complex calcium phosphate salts are the end products of the biological mineralization process. Dicalcium pyrophosphate (DCP, $Ca_2P_2O_7$) is one of the intermediate products in this process [1,4]. Its Ca/P ratio is 1, far less than TCP, that it is potentially biodegradable in comparison to TCP. The biological response for new bone development is quite similar to HA in spite of the low Ca/P ratio [8–10]. With so many benefits, we selected it as a raw material for a new bone substitute.

However, the development of the sintering technique of this DCP ceramic is not that easy. The sintering temperature of DCP is about 1000 °C. The extent of volume reduction during sintering will affect its microstructure and mechanical strength. Also, the cost of the heating facility is rather high in sintering calcium phosphate ceramics in the block form at temperatures higher than 1000 °C. In order to reduce the sintering temperature, to enhance the sinterability and to improve the initial mechanical strength of the developed material, our modification was to add some sintering additives. One of the sodium polyphosphates, $Na_4P_2O_7 \cdot 10H_2O$ was chosen as an ingredient in developing our new product. The pure DCP and some compositions of this ingredient were built up in a disc-shaped block form. The shrinkage during sintering and the mechanical strength were measured by using a dilatometer and Bionix 858 test system, respectively.

2. Materials and experiments

2.1. Material preparation

DCP powder with addition of $Ca_2P_2O_7$ and mean grain size 0.1 μm was used in the experiment. The specific surface area determined by BET analysis is 51 ± 0.2 cm^2/g. Trace elements that might be connected with biocompatibility were detected by atomic absorption analysis. The concentration of the trace elements was much lower than the maximum tolerable level [11].

The DCP powder was mixed with $Na_4P_2O_7 \cdot 10H_2O$ in water and dried at 70 °C for 3 days. The well-mixed and dried cake was ground and sieved into 40–60 meshed particles. The sieved particles were then compacted in a stainless-steel die under a hydrostatic pressure of 270 MPa and a green density of about 60% TD was obtained. The additive, sodium polyphosphate powder as $Na_4P_2O_7 \cdot 10H_2O$, was prepared in a series composition of 1, 2.5, 5, 7.5, 10, 12 and 15 wt.%. A group of the test samples with a stepwise series of composition of the sintering additives, $Na_4P_2O_7 \cdot 10H_2O$, was manufactured in a dense block form which was more feasible for mechanical strength measurement. The prepared green body was placed on a platinum sheet and heated to various temperatures at a heating rate of 3 °C/min in a conventional Ni–Cr coiled furnace, and then maintained for about 1 h after the sintering temperature of 910 °C was reached [12].

2.2. Measurement of mechanical strength

In the compressive mode, a parallel cylinder of the materials was prepared and external load applied so that the specimen was, macroscopically, in a state of uniaxial stress. The height/diameter ratio was lower than a critical value of 2/1 in order to eliminate the possibility of instability (bucking). Due to the anisotropy of the individual grains, the state of stress is not uniaxial at the microscopic level; stress and strain inhomogeneities establish themselves inside the individual grains. However, in the treatment given here, these localized variations were not considered [12].

Bending strength was measured by a four-point loading method using rectangular specimens $5 \times 5 \times 40$ mm, abraded with alumina powder and diamond paste. The lower and upper span lengths were 32 and 16 mm, respectively. The cross-head speed of 0.5 mm/min was used at room temperature. Ten specimens were prepared for each condition to measure the compressive strength and four-point bending strength, respectively [13].

2.3. Specimen characterization

The specimens were characterized by means of a number of techniques including X-ray diffraction (XRD), scanning

electron microscopy (SEM), transmission electron microscopy (TEM) and dilatometry.

The microstructures of the sintered DCP were observed by the scanning electron microscope. The surfaces were coated with a thin layer (2 μm) of carbon after being polished with diamond paste and etching with 48% HF for about 10 s. They were then observed by SEM and analyzed using an energy-dispersive electron probe X-ray microanalyzer. P, Ca and Na were analyzed across the grains and grain boundaries. An electron beam maintained at 2×10^{-10} A was used and X-ray intensities in counts per second (cps) were recorded. The accelerating voltage was 12 kV. Ultra-thin sections for TEM were obtained from the sintered specimen by slicing with a diamond blade saw and ultrasonic cutter. The slices were polished with diamond abrasive to a thickness of 30 μm on the dimple grinder and then mounted on a copper ring. The specimens were finally thinned by an ion-beam-milling. The crystal structure of intergrain material was investigated by a Hitachi-700 STEM instrument operating at 175 kV. Selected area diffraction patterns were recorded with photographic plates. Tilting the crystal from one orientation to another was carried out in the selected area diffraction mode using the double tilt holder.

The optimum sintered temperature and duration were decided according to the analysis result of the dilatometer. A specimen of 5 mm in diameter and 7 mm in length was placed in a dilatometer where the sintered shrinkage curve was recorded on an X–Y pen recorder; X and Y axes were displacement (in terms of linear shrinkage, $\Delta L/L_0$) and temperature, respectively. All crystalline phases existing in the sintered specimens were identified by the X-ray diffractometer. The phase contents in the sintered DCP were detected with the relative intensities of (008) and (132) reflections of $Ca_2P_2O_7$ and $CaNa(PO_3)_3$, respectively [14,15].

3. Results and discussion

3.1. Mechanical strength and microstructures

Figs. 1 and 2 show the compressive strength and four-point bending strength, respectively, of sintered DCP bioceramics

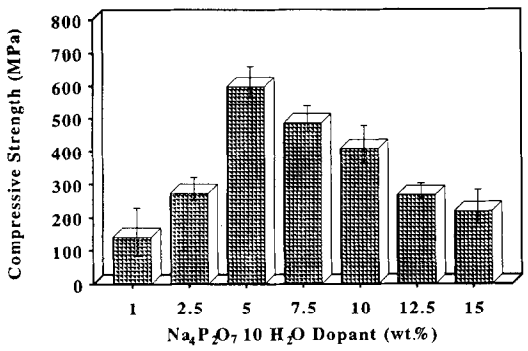

Fig. 1. Compressive strength of sintered DCP on addition of $Na_4P_2O_7\cdot10H_2O$.

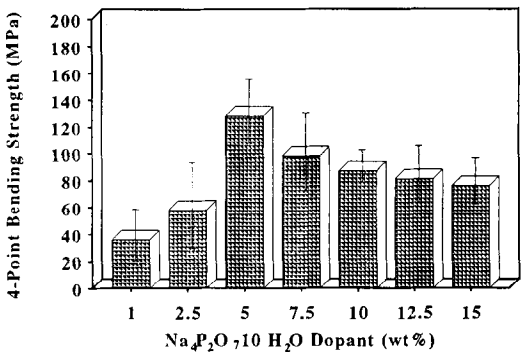

Fig. 2. Four-point bending strength of sintered DCP on addition of $Na_4P_2O_7\cdot10H_2O$.

that were prepared by adding different quantities of $Na_4P_2O_7\cdot10H_2O$. The compressive strength and four-point bending strength of pure DCP bioceramic without addition of $Na_4P_2O_7\cdot10H_2O$ were only 159 MPa and 35 MPa, respectively, which were much lower than those of sintered DCP with 5 wt.% $Na_4P_2O_7\cdot10H_2O$ of addition (589 MPa and 128 MPa). It is obvious that the strength of the DCP dense material initially increased on addition of $Na_4P_2O_7\cdot10H_2O$ up to 5 wt.%, but thereafter decreased.

Densification and growth of the solid particles in the liquid phase sintering have been analyzed by dividing it into three steps [16–18]. (I) The liquid flow or rearrangement stage: on formation of a liquid phase, there is a rearrangement of particles to give a more effective packing. This process can lead to complete densification if the volume of liquid present is sufficient to fill in the interstices completely. In this stage, densification is brought about under the action of capillary pressure by collapse of melt bridges between particles and by arrangement in which solid particles slide over one another. (II) The solution-reprecipitation or accommodation process: in this stage further densification and growth of particles of the solid phase are achieved by solution and reprecipitation and by coalescence process. (III) The solid state sintering stage: in many cases of liquid phase sintering, complete densification is achieved during the first two sintering stages. Prolonged holding of compacts at sintering temperature may lead to microstructural changes in the dense compacts, including further growth of the particles and formation of a rigid skeleton of solid phase in the system (abnormal grain growth) [18].

The microstructure of sintered DCP ceramic containing 2.5 wt.% $Na_4P_2O_7\cdot10H_2O$ is shown in Fig. 3(a). Shackelford [19] assumed that in a brittle material the stress concentration for an infinitesimal extension of the inherent elliptical pore or crack can be expressed as

$$\frac{\sigma_{max}}{\sigma_\infty} = 1 + \frac{2c}{b}$$

For the case of a narrow crack of length c with an elliptical tip whose radius of curvature is r, the above equation can be written as

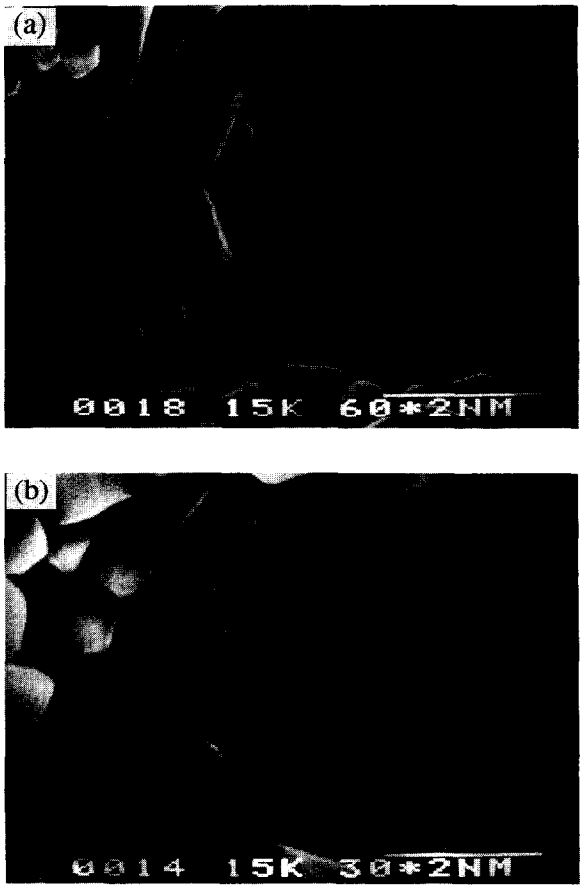

Fig. 3. Microstructure of sintered DCP with addition of (a) 2.5 wt.% and (b) 5 wt.% $Na_4P_2O_7 \cdot 10H_2O$. The former shows a smaller average grain size of about 0.75 μm and remaining pores between the intergranular area. The latter has an average grain size of about 1.3 μm and shows a much more compact microstructure.

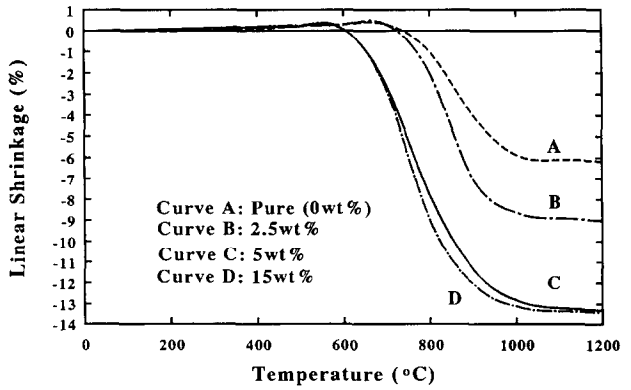

Fig. 4. Sintered linear shrinkage curves of pure sintered DCP and DCP doped with different quantities of $Na_4P_2O_7 \cdot 10H_2O$.

$$\frac{\sigma_{max}}{\sigma_\infty} = 2\left(\frac{c}{r}\right)^{1/2}$$

since $r = b^2/c$ and $c/b \geqslant 1$. For a material, when r becomes atomic scale, the theoretical stress can be approximated by $E/10$, but, if the crack is about 3 μm, the strength becomes $E/1000$. Porosity was seen to remain in the sintered DCP bioceramics with 2.5 wt.% $Na_4P_2O_7 \cdot 10H_2O$ addition. Liquid phase sintering was applied in the sintering process during the addition of $Na_4P_2O_7 \cdot 10H_2O$. However, insufficient $Na_4P_2O_7 \cdot 10H_2O$ was added to DCP, so it was not easy to bring about liquid phase sintering for densification. The average sintered densities for the ceramic were about 85% TD and 91% TD for 1% and 2.5% $Na_4P_2O_7 \cdot 10H_2O$ additions, respectively. In this case, the DCP bioceramics could not densify and remove pores completely. The pores were left inside the material and led to stress concentration around the tips during the material's under loading; thus, a lower mechanical strength was obtained.

The sintered linear shrinkage curves of pure DCP and DCP doped with different quantities of $Na_4P_2O_7 \cdot 10H_2O$ were recorded by the analysis of the dilatometer as shown in Fig. 4. Pure DCP ceramics had the lowest linear shrinkage of only 6%, whereas DCP ceramics doped with up to 5 wt.% $Na_4P_2O_7 \cdot 10H_2O$ demonstrated the greatest linear shrinkage of 13.1%. In Fig. 3(b), the sintered DCP bioceramics with addition of 5 wt.% $Na_4P_2O_7 \cdot 10H_2O$ generally showed a dense and uniform grain size microstructure that corresponded to the higher mechanical strength [17,20]. The sintered DCP bioceramics with addition of 5 wt.% $Na_4P_2O_7 \cdot 10H_2O$ showed a much higher sintered density of about 97.3% TD.

3.2. Effects of grain size on mechanical properties

As seen from Fig. 5, the grain size of sintered DCP increased with the addition of $Na_4P_2O_7 \cdot 10H_2O$. The effect of grain size on the fracture strength has been generally interpreted in terms of the dependence [21]: $\sigma = f(G)^{-1/2}$, where σ is the fracture strength, G is the grain size and f is a proportional constant. Consequently, the larger the grain size of the ceramics, the lower the fracture strength obtained. Moreover, the higher quantities of $Na_4P_2O_7 \cdot 10H_2O$ doped into the DCP bioceramics would speed up atomic diffusion between the grain boundaries and promote the sintered process or densification rate that might lead to the abnormal grain growth or rigid skeleton formation in the sintered system, as shown in Fig. 6. Growth by coalescence in the liquid phase sintering has been repeatedly postulated [16,18]. The process

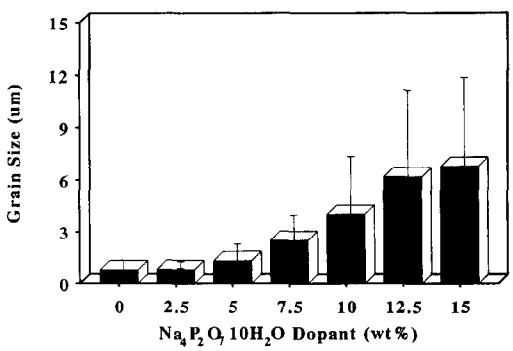

Fig. 5. Mean grain size of sintered DCP bioceramics plotted against the amount of $Na_4P_2O_7 \cdot 10H_2O$.

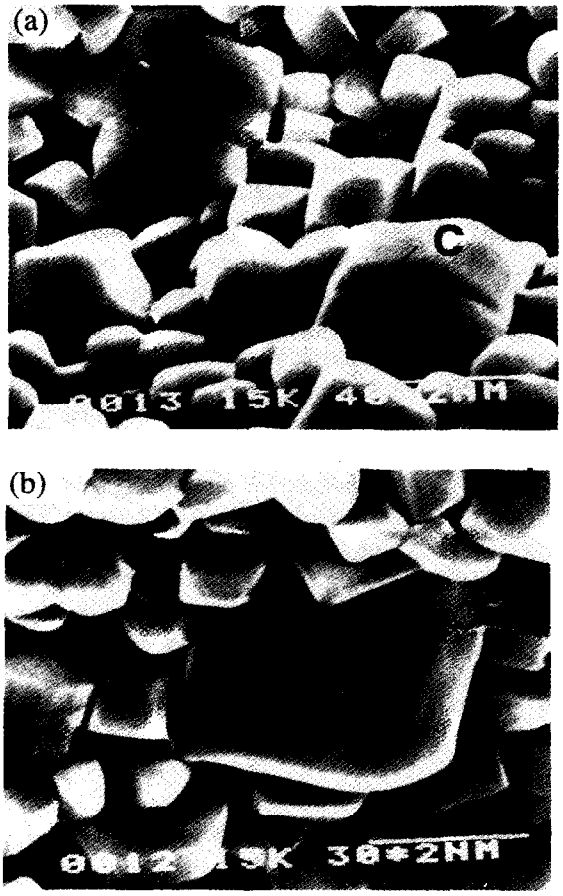

Fig. 6. Microstructure of sintered DCP bioceramics with addition of (a) 7.5 wt.% and (b) 12.5 wt.% $Na_4P_2O_7 \cdot 10H_2O$. The formation of coalescence grains (indicated as C) was observed in the bioceramics with 7.5 wt.% $Na_4P_2O_7 \cdot 10H_2O$ addition where the coalescence line is noted by the arrows. Many abnormal grains (indicated as AG) were examined through the bioceramic with 12.5 wt.% $Na_4P_2O_7 \cdot 10H_2O$ addition.

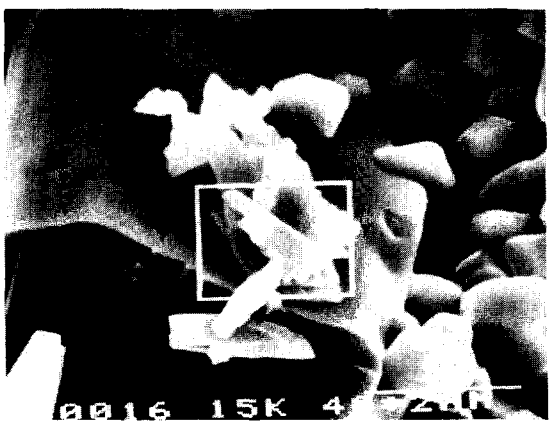

Fig. 7. Micrograph of sintered DCP bioceramics with 15 wt.% $Na_4P_2O_7 \cdot 10H_2O$ addition. A typical fracture due to the stress concentrating on the abnormal grain is shown. The second phase identified as $NaCa(PO_3)_3$ was observed in the matrix which is indicated by NP and arrows.

has also been treated analytically. If the dihedral angle in the sintering system is positive, grain boundaries between coalescence particles will be formed and an aggregate of two, three or more grains will be established. These aggregates may result in the formation of a rigid skeleton or abnormal large grains. Fig. 6(a) shows the microstructure of DCP bioceramics doped with 7.5 wt.% $Na_4P_2O_7 \cdot 10H_2O$, where the coalescence grains and coalescence lines were observed. The microstructure of DCP bioceramics with 12.5 wt.% $Na_4P_2O_7 \cdot 10H_2O$ is shown in Fig. 6(b) and illustrates that the rigid skeleton and abnormally large grains exist in the ceramics. In coarse-grained materials, the stress multiplication in the next grain should be much greater than that in fine-grained materials. This means that in the fine-grained materials a much larger applied stress is needed to cause slip to pass through the boundary than is the case with coarse-grained materials. The stress would concentrate in these abnormally large grains in the specimen under mechanical loading. This stress concentration effect might lead to fracture generating along the abnormally large grains or rigid skeletons. Fig. 7 shows a typical fracture generating along an abnormally large grain in a DCP bioceramic with addition of 15 wt.% $Na_4P_2O_7 \cdot 10H_2O$.

3.3. Crystalline identification

Fig. 8 shows the XRD patterns of sintered DCP bioceramics with different quantities of $Na_4P_2O_7 \cdot 10H_2O$. It is observed that no phase other than DCP is identified below a

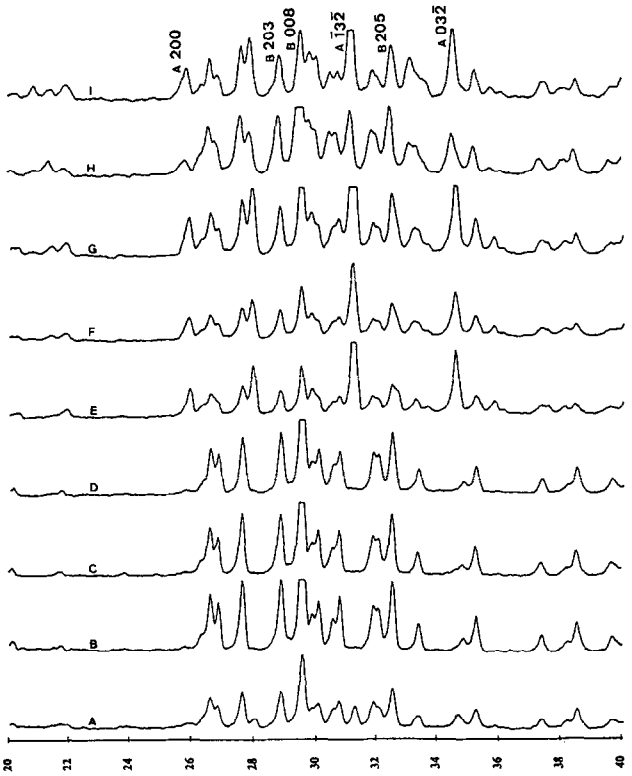

Fig. 8. XRD patterns of sintered DCP with different additions of $Na_4P_2O_7 \cdot 10H_2O$: A, pure DCP sintered at 940 °C; B, pure DCP sintered at 990 °C; C, 1 wt.% addition; D, 2.5 wt.% addition; E, 5 wt.% addition; F, 7.5 wt.% addition; G, 10 wt.% addition; H, 12.5 wt.% addition; I, 15 wt.% addition.

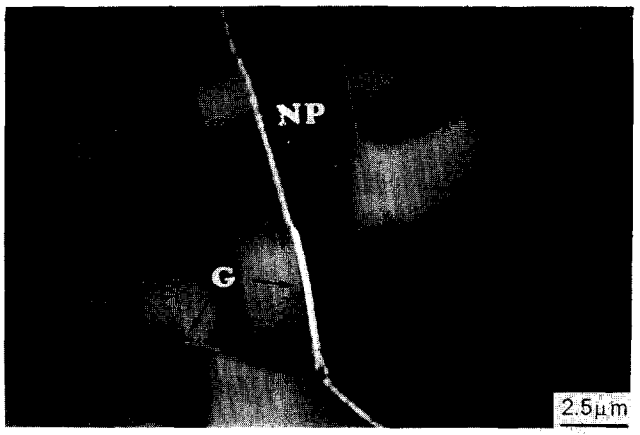

Fig. 9. Transmission electron micrograph of sintered DCP bioceramic with 7.5 wt.% addition of $Na_4P_2O_7 \cdot 10H_2O$ (G: glassy phase; NP: $NaCa(PO_3)_3$).

5 wt.% $Na_4P_2O_7 \cdot 10H_2O$ doping. After addition of 5 wt.% $Na_4P_2O_7 \cdot 10H_2O$, the second phase of $NaCa(PO_3)_3$ is observed where the leading peak of $NaCa(PO_3)_3$ is A(132) as shown in Fig. 8. If R is the ratio of peak height of $NaCa(PO_3)_3$ (A(132)) to that of sintered DCP bioceramics (B(008)), then the larger the value of R, the larger amount of $NaCa(PO_3)_3$ obtained in the matrix. The values of R have an obvious tendency to increase with increasing amount of $Na_4P_2O_7 \cdot 10H_2O$. The existence of a second phase in sintered DCP might lead to the initiation of fracture [13,21]. The glassy phase distributed along the grain boundaries and the second phase was precipitated in the matrix that could be observed from the transmission electron microscope for the sintered DCP bioceramics doped with 7.5 wt.% $Na_4P_2O_7 \cdot 10H_2O$, as shown in Fig. 9. The second phase was identified as the $NaCa(PO_3)_3$ crystal by the selected area diffraction pattern. The spot pattern was (231) orientation of the $NaCa(PO_3)_3$ crystal and was analyzed by the equivalent superimposed projection pattern, as shown in Fig. 10. The $NaCa(PO_3)_3$ crystal was then precipitated as a spindle-shaped grain (Fig. 7) when the $Na_4P_2O_7 \cdot 10H_2O$ addition was increased. The chemical composition of the spindle-shaped grains was measured with electron probe microanalysis–wavelength dispersion spectrophotometer (EPMA–WDS) and was consistent with that of the $NaCa(PO_3)_3$ crystal.

These facts may be summarized as follows: the decrease of mechanical strength of sintered DCP bioceramics after addition of more than 5 wt.% $Na_4P_2O_7 \cdot 10H_2O$ is probably due to the presence of the second phase, increasing grain size and abnormal grain growth.

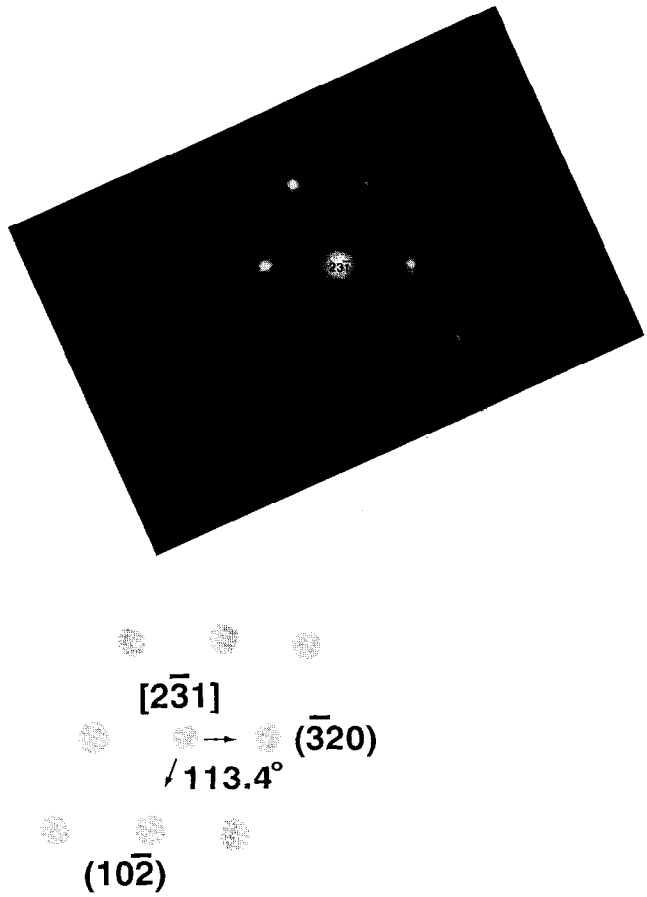

Fig. 10. NP grain indicated on Fig. 9 was identified as $NaCa(PO_3)_3$ crysta in (231) orientation by a selected area diffraction pattern.

after which the trend reversed. Pores, grain size and coales cence large grains, second phase presence, and glassy phas on the grain boundary were speculated as the major fou factors affecting the curve shape of the mechanical strengt plotted against $Na_4P_2O_7 \cdot 10H_2O$ dopant. The pores wer assumed to decrease in size or amount with th $Na_4P_2O_7 \cdot 10H_2O$ addition, which was interpreted as a positive effect to the mechanical strength. The presence of the second phase, grain size and abnormal grain growth, and glassy phase on the grain boundaries, however, increased with the $Na_4P_2O_7 \cdot 10H_2O$ addition, which was supposed to have a negative effect on the mechanical strength. The interaction of these four factors leads the sintered DCP with $Na_4P_2O_7 \cdot 10H_2O$ to have the best mechanical properties at 5 wt.% addition. It is thought to have a great potential in the field of orthopedic application in the near future.

4. Conclusions

The compressive strength and four-point bending strength of sintered DCP bioceramics with addition of $Na_4P_2O_7 \cdot 10H_2O$ initially showed a positive tendency to increase with the amount of $Na_4P_2O_7 \cdot 10H_2O$ up to 5 wt.%,

Acknowledgements

The authors sincerely appreciate the National Science Council (ROC) for their financial support to accomplish the research. We dedicate this research with gratitude to the National Science Council, ROC.

References

[1] P. Ducheyne, *J. Biomed. Mater. Res.: Appl. Biomater., 21A* (1987) 219–236.

[2] R.W. Bucholz and R.E. Holmes, *Orthoped. Clin. North Am., 18* (1987) 323–334.

[3] S.I. Stupp, J.A. Hanson, J.A. Eurell, G.W. Ciegler and A. Johnson, *J. Biomed. Mater. Res., 27* (1993) 301–311.

[4] M. Aebi and P. Regazzoni, *Bone Transplantation, Up-dating on Osteochondral Auto- and Allografting*, Springer, Berlin, 1987.

[5] C.P.A.T. Klein, H.B.M. Lubbe, K. de Groot and A. Hooff, *J. Biomed. Mater. Res., 17* (1983) 769–784.

[6] M. Jarcho, *Clin. Orthop. Relat. Res., 156* (1981) 259–278.

[7] C.P.A.T. Klein, K. de Groot, A.A. Driessen and H.B.M. Lubbe, *Biomaterials, 6* (1985) 189–192.

[8] T. Kitsugi, T. Yamamuro, T. Nakamura, S. Kotani and T. Kokubo, *Biomaterials, 4* (1993) 216–224.

[9] J. Weng, J. Wang and W. Chen, *1st Far-Eastern Symp. Biomedical Materials, Beijing, China, 6–8 Oct. 1993*, p. 153.

[10] F.H. Lin and M.H. Hon, *Ceram. Int., 5* (1989) 530–536.

[11] G.F. Nordberg, *Effects and Dose-relationships of Toxic Metals*, Elsevier, Amsterdam, 1976, p. 48.

[12] F.H. Lin, H.C. Liu, M.H. Hon and C.Y. Wang, *J. Biomed. Eng., 15* (1993) 481–486.

[13] M.A. Meyers and K.K. Chawla, *Mechanical Metallurgy — Principles and Applications*, Prentice-Hall, Englewood Cliffs, NJ, 1984.

[14] D.C. Sheehan and B.B. Hrapchak, *Theory and Practice of Histotechnology*, C.V. Mosby, London, 1980.

[15] F.H. Lin, M.H. Hon and Y.Y. Huang, *Biomed. Eng.: Appl. Basis Commun. (ROC), 2* (1991) 98–106.

[16] F.V. Lenel, *Trans. AIME, 175* (1984) 878–891.

[17] J.F. Shackelford, *Introduction to Materials Sciences and Engineering*, Macmillan, London, 2nd edn., 1990.

[18] D.N. Yoon and W.J. Huppmann, *Acta Metall., 27* (1979) 693–698.

[19] J.F. Shackelford, *Introduction to Materials Science for Engineers*, Macmillan, London, 2nd edn., 1990.

[20] R.W. Davidge, *Mechanical Behavior of Ceramics*, Cambridge Solid State Science Series, Cambridge University Press, Cambridge, 1979.

[21] S.T. Rolfe and J.M. Barson, *Fracture and Fatigue Control in Structures*, Prentice-Hall, Englewood Cliffs, NJ, 1977.